

Multi-messenger constraints on LIGO/Virgo/KAGRA gravitational wave binary black holes merging in AGN disks

T. CABRERA ,¹ A. PALMESE ,¹ AND M. FISHBACH ,²

¹*McWilliams Center for Cosmology, Carnegie Mellon University, 5000 Forbes Avenue, Pittsburgh, PA 15213, USA*

²*Canadian Institute for Theoretical Astrophysics, 60 St George St, University of Toronto, Toronto, ON M5S 3H8, Canada*

ABSTRACT

While the LIGO/Virgo/KAGRA (LVK) gravitational wave (GW) detectors have detected over 300 binary black hole (BBH) mergers to date, the first confirmation of an electromagnetic (EM) counterpart to such an event remains elusive. Previous works have performed searches for counterpart candidates in transient catalogs and have identified active galactic nuclei (AGN) flares coincident with GW events; existing theory predicts that such flares may arise from the interaction of the merger remnant with the embedding accretion disk environment. We apply a statistical formalism to measure the significance of coincidence for the catalog as a whole, measuring that less than 3% (90% credible interval) of LVK BBH mergers give rise to observable AGN flares. This result still allows up to $\sim 40\%$ of BBH mergers to originate in AGN disks. We also examine the individual coincidences of each merger/flare pairing, determining that in all cases the flares are more likely to belong to a background population of flares not associated with GW events. Our results are consistent with theoretical predictions accounting for the observability of EM counterparts in AGN disks, as well as based on the fact that the most massive AGNs (such as those included in the search) are not expected to harbor the majority of the BBHs. We emphasize that developing both the means to distinguish BBH counterpart flares from background AGN flares and an understanding of which BBHs are most likely to produce AGN flares as counterparts is critical to optimize the use of follow-up resources.

1. INTRODUCTION

Ninety gravitational wave (GW) events were reported in the LIGO/Virgo/KAGRA (LVK) GWTC-3 catalog covering the first three observing runs (O1-O3) of the detector network (Abbott et al. 2019, 2021, 2023a,b), and more than 200 additional candidate events have been detected during the ongoing fourth observing run (O4). Over 95% of these events are binary-black hole (BBH) mergers, and much effort has been dedicated to discerning the astrophysical origin of these objects (e.g. Raccaelli et al. 2016; Eldridge & Stanway 2016; Hotokezaka & Piran 2017; Spera et al. 2019; Marchant et al. 2019; Di Carlo et al. 2020; Rodriguez et al. 2021; Mapelli et al. 2021; Callister et al. 2021a,b; Klencki et al. 2021; Godfrey et al. 2023; Karathanasis et al. 2023). Significant discussion is focused on determining the contribution of various formation channels to the overall BBH population, with the current dataset supporting a combination of multiple formation channels (e.g. Arca Sedda et al. 2020; Zevin et al. 2021; Bouffanais et al. 2021; Mapelli et al. 2022; Cheng et al. 2023; Ray et al. 2024).

One such formation channel is the active galactic nucleus (AGN) channel. In this channel, BBHs are formed

from stars and BHs embedded in the accretion disks of AGNs. The gaseous and dusty environment is expected to be one of the best accelerants for BBH formation and inspiral due to the dynamical friction manifested therein (Bartos et al. 2017; Stone et al. 2017; Tagawa et al. 2020b; Ishibashi & Gröbner 2024; Whitehead et al. 2024; Wang et al. 2025). Furthermore, the deep potential wells of the supermassive black holes (SMBHs) located at the centers of AGNs are conducive to retaining previous merger remnants and facilitate hierarchical mergers; such repeated mergers could contribute significantly to the observed high-mass ($> 50 M_{\odot}$) and upper mass gap objects (Doctor et al. 2020; Tagawa et al. 2021; Ford & McKernan 2022; Li 2022; Vaccaro et al. 2024), where a sub-population of mergers is observed (Magaña Hernandez & Palmese 2025; Magaña Hernandez & Palmese 2025a; Antonini et al. 2025; Tong et al. 2025).

A special feature of the AGN formation channel is that it is thought to enable the production of electromagnetic (EM) counterparts following BBH mergers (Bartos et al. 2017; Perna et al. 2018; McKernan et al. 2019; Perna et al. 2019; Wang et al. 2021; Tagawa et al. 2023, 2024; Ma et al. 2024; Chen & Dai 2024; Rodríguez-Ramírez

et al. 2024). The detection of EM counterparts to GW events is the gold standard in the localization of these events; in addition, EM data greatly amplifies the efficacy of analyses using GW data for measurements of key physical parameters such as the Hubble constant (see Palmese & Mastrogiovanni 2025 for a review). To date, only the binary neutron star (BNS) merger GW170817 has been confidently associated with a confirmed counterpart (Abbott 2017), and the latest estimations of BNS or neutron star-black hole multimessenger detection rates are converging towards a handful per year due to the low volumetric rates of these systems (Kunnumkai et al. 2024a,b). On the other hand, despite a growing catalog of BBH alerts, no EM transient has been unequivocally connected to a BBH merger. The most investigated BBH counterpart candidate is associated with the high-mass event GW190521 (Abbott et al. 2020), and occurred roughly 50 days after the LVK trigger (Graham et al. 2020).

Leading models of BBH counterparts involve the interaction of the merger remnant with the AGN disk material, but the particularities of the manifestation of a counterpart are still uncertain. Several models consider the formation of an accretion feedback-driven bubble about the remnant, which then breaks out from the surface of the accretion disk in a flare-like manner (McKernan et al. 2019; Wang et al. 2021; Rodríguez-Ramírez et al. 2024); other works study more extreme possibilities such as that of an accretion-induced jet punching out of the disk (Tagawa et al. 2023, 2024). This diversity of proposed counterpart mechanisms complicates the confirmation of such transients, as a wide variety of timescales and flare morphologies is possible. Confirmation is further complicated by the necessary coincidence of these signals with the inherent variability of the host AGNs. Although the understanding of AGN activity continues to advance, along with possible means to disentangle genuine transients from standard activity, the one-to-one matching of AGN flares to GW events has remained a milestone of future work.

Accepting the present uncertainties in these studies, several BBH counterpart candidates have been proposed by different teams (Connaughton et al. 2016; Greiner et al. 2016; Connaughton et al. 2018; Graham et al. 2020, 2023; Cabrera et al. 2024). One broad search was conducted by Graham et al. (2023), which sifted data from the Zwicky Transient Facility (ZTF) (Bellm et al. 2019) to find AGN flares coincident with GW events from GWTC-3. 7 AGN flares with sufficiently interesting morphology were collectively found in the 90% localization volumes and follow-up windows of 9 GW

events, to the extent that they could not be eliminated as potential counterparts to the respective events.

Although it is challenging to confidently associate AGN flares to individual BBH events, we can better understand the statistical association by considering the population of events. While the AGN flares presented in Graham et al. (2023) have not been definitively identified as EM counterparts, this work undertakes the task of studying the statistical significance of such a dataset as it pertains to the association of LVK BHs with AGN flares. We employ the methods presented in Palmese et al. (2021), and derive posteriors on parameters of interest, specifically the astrophysical fraction λ of BBHs that produce AGN flares, and the association probabilities for each possible GW-AGN pairing. Following the suggestions in the original paper we implement a quasar luminosity function (QLF) (Hopkins et al. 2007) and selection effects to better situate the analysis for observational data, and refine our background AGN flare rate calculations to consider differing AGN flare morphologies. In Section 2 we describe the statistical method used and the assumptions made in the analysis. In Section 3 we present the data used, while in Section 4 we show our results. Sections 5 and 6 include a discussion of our findings and the conclusions from this work, respectively.

2. METHODS

2.1. Statistical framework

The framework of Palmese et al. (2021) considers the coincidence of an observed set of AGN flares in the context of a GW event catalog and an AGN flare background model to investigate the scenario where some flares originate from BBH mergers. In other words, if a fraction of the population of AGN flares observed in coincidence with GW events is indeed related to the compact object mergers, they will follow a different distribution in sky position and redshift compared to the case in which they all arise from some unrelated AGN flaring event. We can statistically constrain that fraction through the method described in Palmese et al. (2021), and we summarize the main components of the inference in what follows.

For a single GW event, there is some spatiotemporal follow-up window wherein a counterpart, if any, is expected to manifest; in other words, there is some volume containing the possible locations of a counterpart, and there is some time interval after the GW event when a counterpart is expected to first become observable. The possible counterparts to the GW event are therefore those that fall in the respective follow-up window. As implementing the temporal part of the window is

simple after a time interval is chosen, we discuss how we handle the spatial window here.

For GW event i , the likelihood of observing k AGN flares at sky positions and redshifts $\{\Omega_{ij}^{\text{AGN}}, z_{ij}^{\text{AGN}}\}_{j=1}^k$ and the GW data x_i^{GW} , given the astrophysical fraction of LVK-observable BBHs that produce AGN flares λ and the AGN flare background rate R_B , is:

$$\begin{aligned} \mathcal{L}_i &\equiv p\left(\{\Omega_{ij}^{\text{AGN}}, z_{ij}^{\text{AGN}}\}_{j=1}^k, x_i^{\text{GW}} | \lambda, R_B\right) \\ &= \int d\Omega_i^{\text{GW}} dz_i^{\text{GW}} p\left(\{\Omega_{ij}^{\text{AGN}}, z_{ij}^{\text{AGN}}\}_{j=1}^k, \Omega_i^{\text{GW}}, z_i^{\text{GW}}, x_i^{\text{GW}} | \lambda, R_B\right) \end{aligned} \quad (1)$$

where in the second line we have marginalized over the uncertain GW sky position Ω_i^{GW} and redshift z_i^{GW} . No more than one flare can be considered to be genuinely produced by the GW event, with the other flares assigned to the background flare population, so that at least $k - 1$ flares are associated to the background.

Assuming that the AGN flares are generated by independent processes, the integrand of the equation above can be expressed using the formalism of an inhomogeneous Poisson process similarly to [Mandel et al. \(2019\)](#):

$$\begin{aligned} p\left(\{\Omega_{ij}^{\text{AGN}}, z_{ij}^{\text{AGN}}\}_{j=1}^k, \Omega_i^{\text{GW}}, z_i^{\text{GW}}, x_i^{\text{GW}} | \lambda, R_B\right) \\ = \prod_{j=1}^k p(x_i^{\text{GW}} | \Omega_i^{\text{GW}}, z_i^{\text{GW}}) p_0(\Omega_i^{\text{GW}}, z_i^{\text{GW}}) \frac{dN}{d\Omega dz} e^{-\mu_i} \end{aligned} \quad (2)$$

$$\mathcal{L}_i \propto \prod_{j=1}^k [\lambda p(\Omega_{ij}^{\text{AGN}}, z_{ij}^{\text{AGN}} | x_i^{\text{GW}}) + R_B(\Omega_j^{\text{AGN}}, z_j^{\text{AGN}})] e^{-\mu_i}. \quad (5)$$

A posterior on the desired parameters, such as λ in this case, can be constructed from the likelihoods for all GW events considered during a follow-up campaign:

$$\begin{aligned} p(\lambda | \{x_i^{\text{GW}}\}_{i=1}^N, \{\{\Omega_{ij}^{\text{AGN}}, z_{ij}^{\text{AGN}}\}_{j=1}^k\}_{i=1}^N, R_B) \\ \propto p(\lambda) \prod_{i=1}^N \mathcal{L}_i. \end{aligned} \quad (6)$$

Note that when calculating the posterior in practice, the likelihoods for GW events without associated AGN flares are simply proportional to the exponential term, and only that factor need be included:

$$\mathcal{L}_{i,\text{flareless}} \propto e^{-\mu_i}. \quad (7)$$

where $p_0(\Omega, z)$ is the prior on the GW event position and $dN/(d\Omega dz)$ is the distribution of AGN flares, which depends on λ and the background rate R_B (the latter in units of flares per steradian per redshift per follow-up), and may be modeled as a mixture of GW counterpart and background source terms:

$$\begin{aligned} \frac{dN}{d\Omega dz}(\Omega, z | \Omega_i^{\text{GW}}, z_i^{\text{GW}}, \lambda, R_B) \\ = \lambda \delta(\Omega_i^{\text{GW}} - \Omega) \delta(z_i^{\text{GW}} - z) + R_B(\Omega, z), \end{aligned} \quad (3)$$

where the δ represent Dirac δ functions. In Eq. 2, μ_i is the expected number of flares associated with the GW event, taking into account the detection probability $P_{\text{det}}^{\text{AGN}}$,

$$\mu_i \equiv \int d\Omega dz P_{\text{det}}^{\text{AGN}}(\Omega, z) \frac{dN}{d\Omega dz}. \quad (4)$$

After performing the integration, the likelihood in Eq. (1) for a single GW event takes the form

The $p(\Omega_{ij}^{\text{AGN}}, z_{ij}^{\text{AGN}} | x_i^{\text{GW}})$ term in the likelihood is simply the posterior probability on Ω and z , estimated using the skymap of the GW event i at the position of the AGN flare j , and priors which are isotropic over the sky and assume a uniform merger rate per comoving volume ([Abbott et al. 2023a](#)); the background AGN flare rate distribution $R_B(\Omega_j^{\text{AGN}}, z_j^{\text{AGN}})$ is constructed from existing models as follows.

2.2. AGN flare background distributions

We deconstruct the background distribution of AGN flares R_B into several components: the physical distribution of AGNs, the rate of flares per AGN, and the follow-up time interval.

The background AGN distribution contributes to our analysis in two spots: once when computing the distribution of flares (Eq. 3), and once when computing the expected number of flares (Eq. 4). In the former case the astrophysical distribution of AGN is most appropriate, and so we use a distribution calculated by applying a <20.5 g -band magnitude cut (the approximate depth of the ZTF survey) to the quasar luminosity function of (Hopkins et al. 2007). In the latter case, the background distribution is multiplied by the detection probability $P_{\text{det}}^{\text{AGN}}$. As we assume all flares in the follow-up windows are detected, the only contribution to $P_{\text{det}}^{\text{AGN}}$ comes from the observability of the AGNs, as flare candidates are only preserved if they match to an observable AGN. We follow the selection criteria of Graham et al. 2023 and use the AGN distribution from the Million Quasars Catalog v7.2 (Flesch 2021) in this case, substituting this distribution for the combined term $P_{\text{det}}^{\text{AGN}} \cdot dN/(d\Omega dz)$. We also experimented with a distribution constructed from assuming a constant comoving volume density of $10^{-4.75}$ AGN/Mpc 3 (Greene & Ho 2007, 2009), and did not observe an appreciable change in results.

Regarding the flare rate per AGN r_{flare} , Graham et al. (2023) calculates an empirical rate of $1.06 \pm 3.73 \times 10^{-8}$ flares per AGN per day. This rate is constructed as the product of the fraction of flares passing each of their selection cuts, and is interpreted as the rate at which AGN produce counterpart-like flares, regardless of the actual generating mechanism. We implement this flare rate in our analysis by sampling a rate from a normal distribution with a mean and standard deviation equal to the rate and uncertainty given by Graham et al. (2023), truncated at $r_{\text{flare}} < 0$ to ensure a non-negative rate. We marginalize over this parameter in our final results.

The follow-up time interval used by Graham et al. (2023) is 200 days, and so we carry this value forward to our analysis.

In summary, we calculate the volumetric flare rate per GW follow-up R_B in Eq. 3 as

$$R_B(z) = \frac{1}{4\pi \text{ sr}} \cdot \frac{dN_{\text{AGN}}}{dz}(z) \cdot r_{\text{flare}} \cdot 200 \text{ days}, \quad (8)$$

where r_{flare} is in units of flares per AGN per time. For simplicity we assume the background rate is isotropic over the sky, including the factor of $1/(4\pi \text{ sr})$ so R_B is the volumetric rate of flares per follow-up.

3. DATA

We use GWTC-3.0 (Abbott et al. 2023a,b) and the AGN flare dataset of Graham et al. (2023) to derive posteriors on the BBH-AGN association fraction λ for the different models. Graham et al. (2023) identified 7

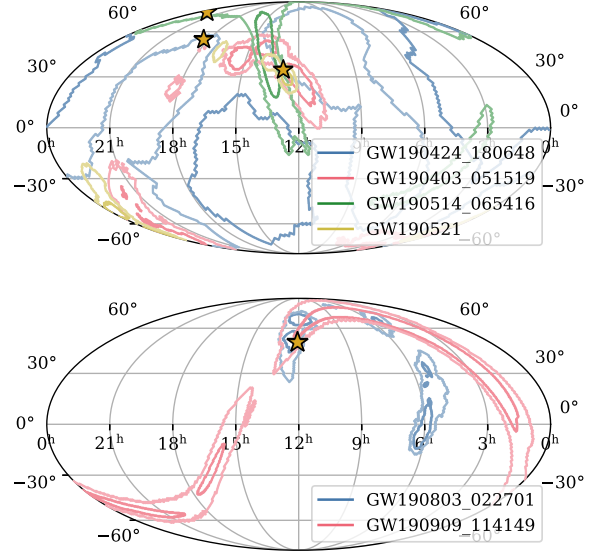


Figure 1. The spatial correlations of the GW events and AGN flares considered in this study. Each subplot contains all flares associated with the depicted GWs, and all GWs associated with the depicted flares. GWs are plotted including the 2D 50% and 90% contours (with the 50% contour being the darker of the two). Flares are plotted as stars.

flares in their ZTF dataset that met the selection criteria for GW merger counterpart candidacy; these cuts included selections on flare morphology, energetics, and naturally proximity to high-probability regions of the GW skymaps.

We exclude a few GW-flare associations reported by Graham et al. 2023 in our analysis. The flare J053408.41+085450.6 is excluded due to an increased likelihood of arising from blazar activity; Graham et al. 2023 already noted this possibility due to the radio signature of the host, and ZTF long-term monitoring of this object reveals blazar-like activity since 2023. Excluding this flare also leads to the removal of GW190731_170936 from the list of possible multimessenger events, as the respective flare was the only possible counterpart to the event. In addition, the GW-flare crossmatch routine we use¹ does not reproduce some of the GW-flare associations found in Graham et al. 2023, as some flares were located on the threshold of the 90%

¹ When performing our crossmatching, we use a custom version of `ligo.skymap.postprocessing.crossmatch.crossmatch`, which has been modified to enable the specification of different cosmologies.

Table 1. Parameters for the gravitational wave events used in this study, reproduced from Abbott et al. 2021, 2023a.

Event ID	90% Area	d_L	m_1	m_2	m_{fin}	χ_{eff}
	deg 2	Mpc	M_{\odot}	M_{\odot}	M_{\odot}	
GW190403_051519	3900	8280 $^{+6720}_{-4290}$	85 $^{+27.8}_{-33}$	20 $^{+26.3}_{-8.4}$	102.2 $^{+26.3}_{-24.3}$	0.68 $^{+0.16}_{-0.43}$
GW190424_180648	28000	2200 $^{+1580}_{-1160}$	40.5 $^{+11.1}_{-7.3}$	31.8 $^{+7.6}_{-7.7}$	68.9 $^{+12.5}_{-9.7}$	0.13 $^{+0.22}_{-0.22}$
GW190514_065416	3000	3890 $^{+2610}_{-2070}$	40.9 $^{+17.3}_{-9.3}$	28.4 $^{+10}_{-10.1}$	66.4 $^{+19}_{-11.5}$	-0.08 $^{+0.29}_{-0.35}$
GW190521	1000	3310 $^{+2790}_{-1800}$	98.4 $^{+33.6}_{-21.7}$	57.2 $^{+27.1}_{-30.1}$	147.4 $^{+40}_{-16}$	-0.14 $^{+0.5}_{-0.45}$
GW190803_022701	1500	3190 $^{+1630}_{-1470}$	37.7 $^{+9.8}_{-6.7}$	27.6 $^{+7.6}_{-8.5}$	62.1 $^{+11.2}_{-7.6}$	-0.01 $^{+0.23}_{-0.28}$
GW190909_114149	4700	3770 $^{+3270}_{-2220}$	45.8 $^{+52.7}_{-13.3}$	28.3 $^{+13.4}_{-12.7}$	72.0 $^{+54.9}_{-16.8}$	-0.06 $^{+0.37}_{-0.36}$

Table 2. Parameters for the AGN flares used in this study. Host redshifts are reproduced from Graham et al. 2023. Onset dates t_0 are calculated as $t_{\text{peak}} - 3\sigma_{\text{rise}}$, where the two parameters are taken from fitting a Gaussian rise-exponential decay model to the flare profile (Graham et al. 2023): t_{peak} is the fit time of flare maximum, and σ_{rise} is the fit standard deviation of the Gaussian rise.

Event ID	Redshift	t_0
J124942.30+344928.9	0.438	2019-06-08
J181719.94+541910.0	0.234	2019-08-08
J224333.95+760619.2	0.353	2019-07-15
J120437.98+500024.0	0.389	2019-12-15

CI volumes for the respective GW events. For self-consistency we remove these threshold cases, resulting in the exclusion of the associations among the flares J154342.46+461233.4 and J183412.42+365655.3 and the GW events GW200216_220804 and GW200220_124850.

This leaves us with a narrowed selection of 6 GW events and 4 AGN flares, among which there are 8 as-

sociations. Relevant parameters for these phenomena are represented in Tables 1 and 2, and skymaps of the events are plotted in Figure 1.

4. RESULTS

4.1. Fiducial analyses

The resulting posteriors on λ are displayed in Figure 2; in our fiducial analysis we find that the posterior probability is maximized for $\lambda = 0$, with a 90% highest-probability upper limit of $\lambda < 2.8\%$. We run the same analysis considering only the BBHs coincident with flares (6, versus the complete GWTC-3.0 catalog of 83), and derive a 90% upper limit of $\lambda < 39.5\%$. This limit is derived to understand the significance of the contribution of the events with no EM flare association to the tight $\sim 3\%$ constraint (we perform additional analysis to investigate the dependence of the posterior on BBH mass and AGN luminosity; see §4.2).

We additionally combine the terms from Eq. 5 to produce association probabilities describing the relative probability that a flare is caused by a particular BBH merger. For a GW event i and an AGN flare j , we calculate the association probability as

$$p_{ij}^{\text{GW-AGN}} = \frac{\lambda p(\Omega_{ij}^{\text{AGN}}, z_{ij}^{\text{AGN}} \mid d_i^{\text{GW}})}{\sum_i (\lambda p(\Omega_{ij}^{\text{AGN}}, z_{ij}^{\text{AGN}} \mid d_i^{\text{GW}})) + R_B(\Omega_j^{\text{AGN}}, z_j^{\text{AGN}})}, \quad (9)$$

where $p(\Omega_{ij}^{\text{AGN}}, z_{ij}^{\text{AGN}} \mid d_i^{\text{GW}})$ and R_B are calculated as in Eq. 5. This statistic weighs the flare j - GW event i association against all other possible sources for that

flare, including any other coincident GW events and the background flare distribution. We also calculate

$$p_j^{\text{BG-AGN}} = \frac{R_B(\Omega_j^{\text{AGN}}, z_j^{\text{AGN}})}{\sum_i (\lambda p(\Omega_{ij}^{\text{AGN}}, z_{ij}^{\text{AGN}} \mid d_i^{\text{GW}})) + R_B(\Omega_j^{\text{AGN}}, z_j^{\text{AGN}})}, \quad (10)$$

which represents the relative probability that the flare j came from the AGN background and not from the GW event of interest.

The posterior PDFs on these association probabilities are plotted in Fig. 3, in a grid mapping the possible GW event-AGN flare pairings, with the background origin case plotted in the rightmost column. We calculate $p_{ij}^{\text{GW-AGN}}$ and $p_j^{\text{BG-AGN}}$ in two cases: one where we consider our inferred λ posterior from our analysis including all 83 BBHs (substituting it for λ in Eqs. 9 and 10), and one where we set $\lambda = 0.2$ (vertical dashed lines). The $\lambda = 0.2$ value is a choice motivated by the findings of theoretical predictions: Ford & McKernan (2022) find that 25-80% of LVK BBH mergers could be originating in the disks of AGNs, while Gayathri et al. (2023) find that the fraction should be about 20%. We only expect a fraction of those events to give rise to *observable* EM counterparts, even if they originate in AGN disks, since the remnant may be kicked away from the observer, a jet may not form, the jet may be pointed away from the observer, or the flare may be obscured by the AGN dust. The fraction of the BBH mergers in AGN disks that gives rise to EM emission will depend on the still uncertain EM radiation mechanism. Therefore, 20% should be regarded as an upper limit for our value of λ , which in this work refers to the fraction of BBH mergers that give rise to detectable EM flares.

4.2. Auxiliary analyses

We also calculate the λ posterior for sub-populations of our sample, applying different cuts for BH masses and AGN luminosity; these posteriors are also plotted in Figure 2. Considering $40 M_\odot$ as a threshold mass between “low” and “high” mass BHs, we run our analysis using only the GW events with heaviest median component mass $m_1 < 40 M_\odot$, and then for events with $m_1 > 40 M_\odot$; we also run the analysis in a similar manner for events with median final mass $m_{\text{fin}} < 40 M_\odot$ and then those with $m_{\text{fin}} > 40 M_\odot$. The reason behind the choice of this cut is twofold. First, black holes in the upper mass gap are more likely to originate from hierarchical mergers than isolated binaries, with the pair-instability supernova mass gap recently identified to be within $40 - 50 M_\odot$ (Magaña Hernandez & Palmese 2025b; Antonini et al. 2025; Tong et al. 2025), and predictions indeed showing that the AGN formation channel is expected to significantly contribute to the merger rate of binaries with $m_1 > 40 M_\odot$ (Gayathri et al. 2021). Second, all of the GW events associated with an AGN flare have a primary mass with significant support above this threshold, with a median above it or slightly below. For what concerns the final mass cut,

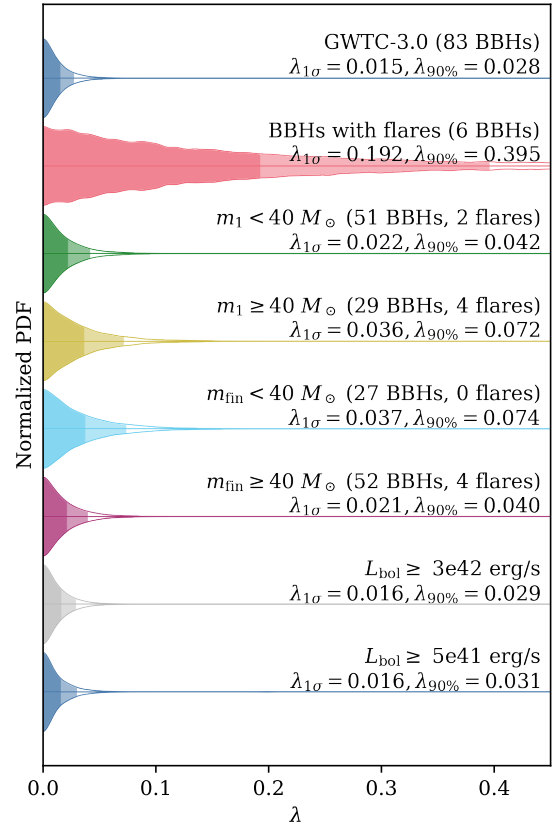


Figure 2. The posterior distributions on the flare production fraction λ for LVK BBH mergers. The 1σ and 90% upper limit regions are shaded, with the respective thresholds labeled. The first posterior (dark blue) is the fiducial analysis, utilizing all 83 BBHs from GWTC-3.0 and applying an $m_g < 20.5$ cut to select AGN observable by ZTF. The second posterior (pink) uses only the 6 BBHs with coincident AGN flares, excluding the information provided by BBHs with no candidate counterparts. The third through sixth posteriors (green, yellow, light blue, purple) use BBHs passing the specified mass cuts. The seventh and eighth posteriors (gray and dark blue) include all BBHs, but select AGN by bolometric luminosity L_{bol} instead of apparent magnitude.

this choice is based on splitting into two the bimodal distribution of final masses from GWTC-3 and the fact that it would include all of the BBH mergers with an associated flare. Given these arguments, it is reasonable to ask whether a different sub-population of BBHs would allow for a larger fraction of events to produce AGN flares; in other words, whether flares are indeed more frequent at higher masses or whether the associations are simply more likely due to the typically larger comoving volumes encompassed by higher mass events (which tend to be detected at larger distances). In all cases, we find that the number of BBHs used for the analysis has the highest impact on the posterior, and

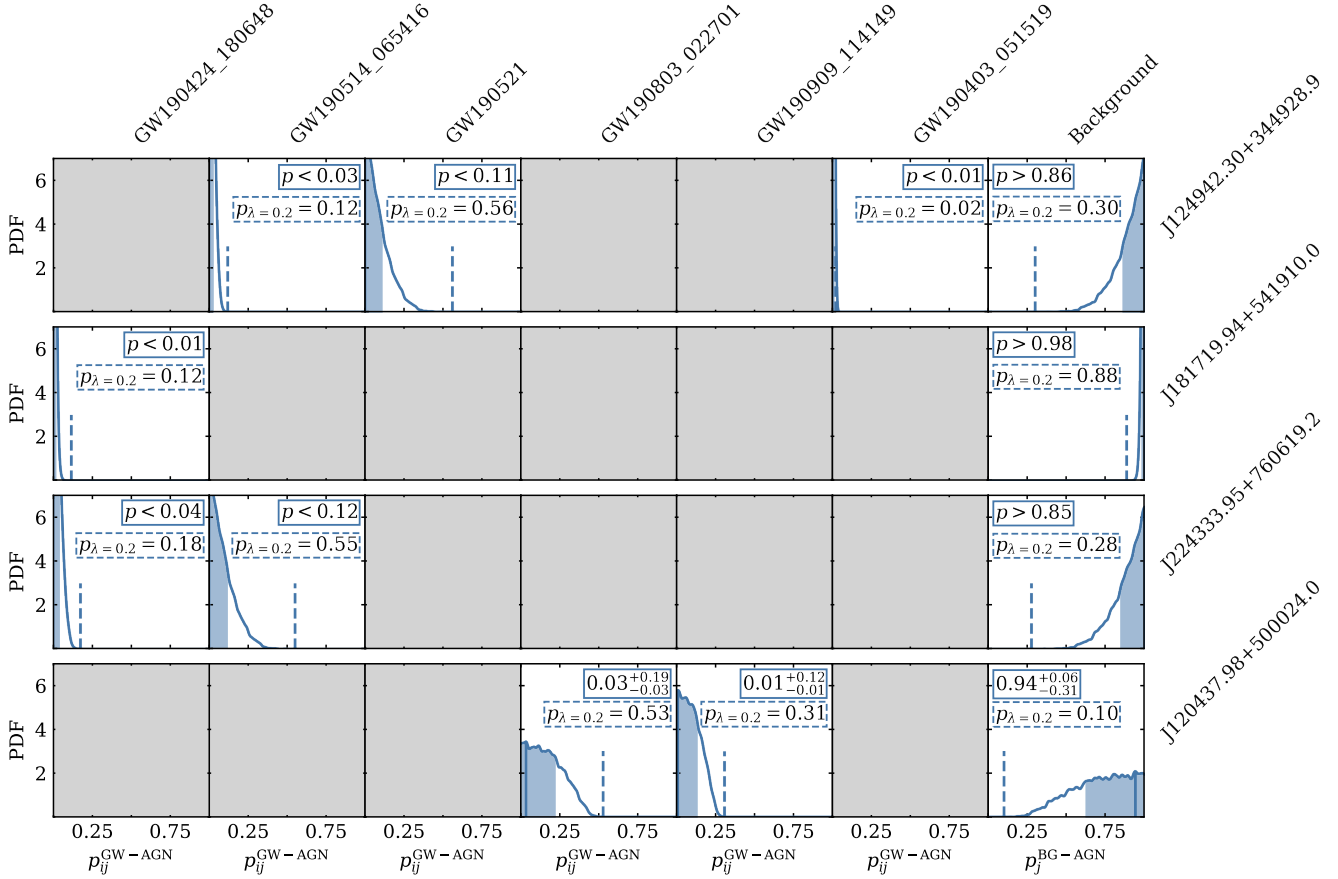


Figure 3. Posteriors on the probability of association for individual GW-flare pairings. The subplots for the associations suggested by [Graham et al. \(2023\)](#) show the respective posterior PDFs; all other subplots are grayed out. Note that the rightmost column plots a comparable, but slightly different statistic (cf. Eqs. 9 and 10). The 1σ upper limit regions are shaded, with the values printed and outlined in a solid box. The respective probabilities in the $\lambda = 0.2$ case are plotted as dashed lines, with the respective values printed above.

not the number of flare-coincident GWs in the sample or the BH masses; for example, the posteriors for the $m_1 > 40 M_\odot$ and the $m_{\text{fin}} < 40 M_\odot$ were nearly identical, with the cuts selecting, respectively, 29 and 27 GW events but the former including all of the GWs with possible flares while the latter cut included none. In other words, we do not find evidence that the high mass subpopulation of mergers accommodates more frequent AGN flares.

To investigate the dependence of λ on AGN luminosity, we first take the AGN mass predicted to produce the most BBH mergers from [Rowan et al. 2024a](#), specifically $M_{\text{SMBH}} = 10^7 M_\odot$. We then convert this mass into luminosity via the AGN mass-luminosity relationships in [Wandel et al. 1999](#) and [Kaspi et al. 2000](#), and calculate the λ posterior including background AGN more luminous than the respective values and fold in our AGN selection function. Because the final constraints are domi-

nated by the large number of non-detections, the resulting λ posteriors are largely the same as those from our fiducial analysis despite the significant ($\sim 1 - 2$ order of magnitude) change in background AGN density at the redshifts of interest ($z \sim 0.2 - 0.6$).

5. DISCUSSION

Our posterior on λ is consistent with the $\lambda = 0$ case, and leads to the expectation that $< 3\%$ of LVK BBHs produce detectable AGN flares as counterparts, given the ZTF observations and the GWTC-3 catalog. This is not surprising in light of the findings of [Graham et al. \(2023\)](#). Assuming that $\sim 50\%$ of LVK BBH mergers arise in AGN disks, that roughly half of the merger remnants are kicked away from the observer (therefore any EM radiation would be unlikely to reach us through the optically thick disk), and that about half of the AGNs are unobscured, they calculated an expected number of

flares from BBH mergers of ~ 3 , corresponding to less than $\sim 4\%$ of the GWTC-3 events under consideration. With a similar reasoning, we can see that even if 40% of LVK BBH mergers arise in AGN disks, we can get a value of λ consistent with our upper limit. In other words, our constraint still allows for the possibility that $\lesssim 40\%$ of LVK BBH events originate in the disks of AGNs.

The association probability posteriors in Fig. 3 aid in the evaluation of causality in the case of particular multimessenger GW-flare pairings. At the broadest level, it can be seen that none of the associations is strongly preferred, with the flare J181719.94+541910.0 strongly preferring the background origin case ($p_j^{\text{BG-AGN}} > 0.98$ at the 1σ level), and the $p_j^{\text{BG-AGN}}$ distributions for all other flares also peaking at 1.

In pursuit of causal connections, the most likely multimessenger pairing is GW190803_022701 - J120437.98+500024.0 ($p_{ij}^{\text{GW-AGN}} < 0.19$). The GW event has component masses (m_1, m_2) of $(37.3_{-7.0}^{+10.6}, 27.3_{-8.2}^{+7.8}) M_\odot$ and an effective spin χ_{eff} of $-0.03_{-0.27}^{+0.24}$ (Abbott et al. 2021, 2023a). Notably, these parameters are favorable for the AGN origin case. The component BHs are of masses appropriate for compact objects merging in AGN disks, which are typically expected to contribute to the $\sim 30 M_\odot$ feature in the mass distribution of BBHs and above (Gayathri et al. 2021; McKernan et al. 2024; Rowan et al. 2024b) more than to the $\sim 10 M_\odot$ feature. Moreover, the marginally negative effective spin could be indicative of a dynamical formation channel in an environment that accelerates the merger process to outpace spin alignment, and can occur in AGN disks (McKernan et al. 2022); this however must be tempered by considering other works that predict that AGN disks can encourage spin alignment for embedded BBHs (Tagawa et al. 2020a; Li et al. 2022; Vaccaro et al. 2024). When evaluating these coincidences one should be mindful that the background flare case is still preferred ($p_{ij}^{\text{GW-AGN}} < 19\%$).

6. CONCLUSIONS

In this work we apply the BBH-AGN association formalism of Palmese et al. (2021) and apply it to the AGN flare GW counterpart candidates of Graham et al. (2023). In doing so we measure the fraction of observed LVK GW events that produce detectable AGN flares λ , finding that less than 3% of events produce flares with 90% confidence. This result still leaves open the possibility that $\lesssim 40\%$ of LVK BBH mergers originate in AGN disks. In addition we examine the particular pairings of GW events to AGN flares, and identify the most likely pairing as GW190803_022701 - J120437.98+500024.0,

albeit the probabilities of association remains less than 20%. We also note that this GW event has BH masses and a χ_{eff} that could be appropriate for the AGN formation channel.

Altogether, our results indicate that multimessenger LVK BBH mergers with AGN flares as counterparts are rare, with likely less than one merger in ~ 40 producing a counterpart of this type. Our findings also indicate that the majority of candidate counterparts to BBH events are actually due to AGN activity unrelated to the GW event (e.g. explosive events breaking out from within the disk or disk instabilities close to the SMBH innermost stable circular orbit; Graham et al. 2023), supporting the need for the inclusion of a background population of AGN flares when associating them to BBH mergers, as well as motivating follow up observations of those to clarify their origin and better characterize their occurrence rates. Moreover, we find no compelling evidence for high mass mergers to be more likely to be associated with the available AGN flares, indicating that the fact that most AGN flares are associated with high mass events may be due to chance coincidences.

Some caveats exist for this measurement, primarily concerning the completeness of the AGN flare sample: First, since models for BBH counterparts have not converged on a consistent phenomenology, it is unknown whether the ZTF data is deep enough to detect all GW-originated flares. In addition, the AGN catalogs used to identify AGN-hosted flares have some degree of incompleteness, and so even if a genuine counterpart was observed it may have been discarded because the host lacks identification. Either case implies that faint flares or flares with faint hosts are not included in the current counterpart candidate sample. The respective effects on the inferred parameters is similarly obscured at this time, as it is unknown whether increasing completeness would recover a proportionally larger amount of GW counterpart or background flares. At any rate, at this point we can only claim that less than a few percent of LVK BBHs produce the bright flares observed in the existing AGN catalogs, which are biased towards the brightest objects, and that deeper follow-up and catalogs are required to extend the limits of these kinds of analyses. This line of thought has some synergy with existing theory, as multiple teams have predicted that BBH mergers and counterpart observability are hampered as central BH mass increases (McKernan et al. 2019; Rodríguez-Ramírez et al. 2024; Delfavero et al. 2024). Note that Rowan et al. (2024b) predict that the majority of BBH mergers in AGN disks should occur around SMBHs of $\sim 10^7 M_\odot$, a sweet spot between the rare, high-mass AGNs and the small numbers of BHs

around dwarf AGNs. The flaring AGNs in [Graham et al. \(2023\)](#) are all $\gtrsim 10^8 M_\odot$, which is reasonable since most AGNs in Milliquas are biased towards the most luminous and massive AGNs. It is therefore possible that the AGNs targeted as part of this search were not associated to the GW events in question, but this does not imply that the BBH mergers did not originate in AGN disks nor that there was no EM counterpart produced. These findings highlight the need to produce AGN catalogs that include objects down to masses of $\lesssim 10^7 M_\odot$, and extend GW follow up campaigns to include such objects.

To enable the best use of observing resources, more effort must be dedicated toward elevating the rate of counterparts per follow-up by making proficient use of the GW event data. Current theories predict that flare energies and timescales depend on the mass of the remnant BH (e.g. [Rodríguez-Ramírez et al. 2024](#)), but the nature of the relationship varies for different flaring mechanisms. Such a miasma of possibilities is difficult to overcome, but a clearer path forward is possible if flare models are developed in particular consideration of GW observables such as chirp mass and spin. Of course, such tools would be particularly useful if low-latency spin estimations were made available in the initial GW alert stream along with chirp masses, and so progress in this direction must be made in concert to enable the community to perform the best science possible. Advancing along these two joined paths will greatly reduce the cost of discovering the first BBH counterpart, or associatively gathering enough evidence that such a possibility can be excluded.

While dedicated BBH follow-up is challenged by our results, survey and archival counterpart searches such as that of [Graham et al. \(2023\)](#) retain promise of being important probes of multimessenger BBHs. The number of GW-observed BBHs has roughly tripled during O4 so far, and so one can expect that a similar sample of AGN flares as the one studied here will be discernible from contemporary data. Such a composite dataset will be useful in analyses such as these to further constrain the nature of BBH counterparts, which will help enable the dedicated follow-up mentioned above. Looking toward the future, the overlap of the Rubin Observatory Legacy Survey of Space and Time (LSST) and LVK O5 will provide a wealth of new information, with LSST probing several magnitudes deeper than ZTF through a dedicated program for BBH mergers follow-up ([Andreoni et al. 2024](#)), and with O5 predicted to detect mergers at roughly ten times the rate of O4. Such large datasets will be all the more suited for statistical analyses relying on a representative sample of events, and will enable additional science. In particular, the method of [Palmese et al. \(2021\)](#) employed here has also been shown to probe cosmological parameters such as the Hubble constant H_0 through a statistical standard siren method; while the present work with its uncertain associations between GWs and AGN flares does not possess sufficient information for significant constraints, the breadth of future datasets are expected to alleviate this deficiency ([Bom & Palmese 2024](#)) and allow steps towards resolving open questions in the field.

REFERENCES

Abbott, B. P. e. a. 2017, *The Astrophysical Journal*, 848, L12, doi: [10.3847/2041-8213/aa91c9](https://doi.org/10.3847/2041-8213/aa91c9)

Abbott, B. P. e. a., LIGO Scientific Collaboration, & Virgo Collaboration. 2019, *Physical Review X*, 9, 031040, doi: [10.1103/PhysRevX.9.031040](https://doi.org/10.1103/PhysRevX.9.031040)

Abbott, R. e. a., LIGO Scientific Collaboration, & Virgo Collaboration. 2020, *Physical Review Letters*, 125, 101102, doi: [10.1103/PhysRevLett.125.101102](https://doi.org/10.1103/PhysRevLett.125.101102)

—. 2021, *Physical Review X*, 11, 021053, doi: [10.1103/PhysRevX.11.021053](https://doi.org/10.1103/PhysRevX.11.021053)

Abbott, R. e. a., Ligo Scientific Collaboration, V. C., & Kagra Collaboration. 2023a, *Physical Review X*, 13, 041039, doi: [10.1103/PhysRevX.13.041039](https://doi.org/10.1103/PhysRevX.13.041039)

—. 2023b, *Physical Review X*, 13, 041039, doi: [10.1103/PhysRevX.13.041039](https://doi.org/10.1103/PhysRevX.13.041039)

Andreoni, I., Margutti, R., Banovetz, J., et al. 2024, arXiv e-prints, arXiv:2411.04793, doi: [10.48550/arXiv.2411.04793](https://doi.org/10.48550/arXiv.2411.04793)

Antonini, F., Romero-Shaw, I., Callister, T., et al. 2025, Gravitational waves reveal the pair-instability mass gap and constrain nuclear burning in massive stars. <https://arxiv.org/abs/2509.04637>

Antonini, F., Romero-Shaw, I. M., & Callister, T. 2025, *PhRvL*, 134, 011401, doi: [10.1103/PhysRevLett.134.011401](https://doi.org/10.1103/PhysRevLett.134.011401)

Arca Sedda, M., Mapelli, M., Spera, M., Benacquista, M., & Giacobbo, N. 2020, *The Astrophysical Journal*, 894, 133, doi: [10.3847/1538-4357/ab88b2](https://doi.org/10.3847/1538-4357/ab88b2)

Astropy Collaboration, Robitaille, T. P., Tollerud, E. J., et al. 2013, *Astronomy and Astrophysics*, 558, A33, doi: [10.1051/0004-6361/201322068](https://doi.org/10.1051/0004-6361/201322068)

Astropy Collaboration, Price-Whelan, A. M., Sipőcz, B. M., et al. 2018, *The Astronomical Journal*, 156, 123, doi: [10.3847/1538-3881/aabc4f](https://doi.org/10.3847/1538-3881/aabc4f)

Astropy Collaboration, Price-Whelan, A. M., Lim, P. L., et al. 2022, *The Astrophysical Journal*, 935, 167, doi: [10.3847/1538-4357/ac7c74](https://doi.org/10.3847/1538-4357/ac7c74)

Bartos, I., Kocsis, B., Haiman, Z., & Márka, S. 2017, *The Astrophysical Journal*, 835, 165, doi: [10.3847/1538-4357/835/2/165](https://doi.org/10.3847/1538-4357/835/2/165)

Bellm, E. C., Kulkarni, S. R., Graham, M. J., et al. 2019, *Publications of the Astronomical Society of the Pacific*, 131, 018002, doi: [10.1088/1538-3873/aaecbe](https://doi.org/10.1088/1538-3873/aaecbe)

Bom, C. R., & Palmese, A. 2024, *Physical Review D*, 110, 083005, doi: [10.1103/PhysRevD.110.083005](https://doi.org/10.1103/PhysRevD.110.083005)

Bouffanais, Y., Mapelli, M., Santoliquido, F., et al. 2021, *Monthly Notices of the Royal Astronomical Society*, 507, 5224, doi: [10.1093/mnras/stab2438](https://doi.org/10.1093/mnras/stab2438)

Cabrera, T., Palmese, A., Hu, L., et al. 2024, *Physical Review D*, 110, 123029, doi: [10.1103/PhysRevD.110.123029](https://doi.org/10.1103/PhysRevD.110.123029)

Callister, T. A., Farr, W. M., & Renzo, M. 2021a, *The Astrophysical Journal*, 920, 157, doi: [10.3847/1538-4357/ac1347](https://doi.org/10.3847/1538-4357/ac1347)

Callister, T. A., Haster, C.-J., Ng, K. K. Y., Vitale, S., & Farr, W. M. 2021b, *The Astrophysical Journal*, 922, L5, doi: [10.3847/2041-8213/ac2ccc](https://doi.org/10.3847/2041-8213/ac2ccc)

Chen, K., & Dai, Z.-G. 2024, *The Astrophysical Journal*, 961, 206, doi: [10.3847/1538-4357/ad0fdf](https://doi.org/10.3847/1538-4357/ad0fdf)

Cheng, A. Q., Zevin, M., & Vitale, S. 2023, *ApJ*, 955, 127, doi: [10.3847/1538-4357/aced98](https://doi.org/10.3847/1538-4357/aced98)

Connaughton, V., Burns, E., Goldstein, A., et al. 2016, *The Astrophysical Journal*, 826, L6, doi: [10.3847/2041-8205/826/1/L6](https://doi.org/10.3847/2041-8205/826/1/L6)

—. 2018, *The Astrophysical Journal*, 853, L9, doi: [10.3847/2041-8213/aaa4f2](https://doi.org/10.3847/2041-8213/aaa4f2)

Delfavero, V., Ford, K. E. S., McKernan, B., et al. 2024, McFacts III: Compact binary mergers from AGN disks over an entire synthetic universe, arXiv, doi: [10.48550/arXiv.2410.18815](https://doi.org/10.48550/arXiv.2410.18815)

Di Carlo, U. N., Mapelli, M., Giacobbo, N., et al. 2020, *Monthly Notices of the Royal Astronomical Society*, 498, 495, doi: [10.1093/mnras/staa2286](https://doi.org/10.1093/mnras/staa2286)

Doctor, Z., Wysocki, D., O'Shaughnessy, R., Holz, D. E., & Farr, B. 2020, *The Astrophysical Journal*, 893, 35, doi: [10.3847/1538-4357/ab7fac](https://doi.org/10.3847/1538-4357/ab7fac)

Eldridge, J. J., & Stanway, E. R. 2016, *Monthly Notices of the Royal Astronomical Society*, 462, 3302, doi: [10.1093/mnras/stw1772](https://doi.org/10.1093/mnras/stw1772)

Flesch, E. W. 2021, *The Million Quasars (Milliquas) v7.2 Catalogue*, now with VLASS associations. The inclusion of SDSS-DR16Q quasars is detailed, arXiv, doi: [10.48550/arXiv.2105.12985](https://doi.org/10.48550/arXiv.2105.12985)

Ford, K. E. S., & McKernan, B. 2022, *Monthly Notices of the Royal Astronomical Society*, 517, 5827, doi: [10.1093/mnras/stac2861](https://doi.org/10.1093/mnras/stac2861)

Gayathri, V., Wysocki, D., Yang, Y., et al. 2023, *The Astrophysical Journal*, 945, L29, doi: [10.3847/2041-8213/acbf8](https://doi.org/10.3847/2041-8213/acbf8)

Gayathri, V., Yang, Y., Tagawa, H., Haiman, Z., & Bartos, I. 2021, *The Astrophysical Journal*, 920, L42, doi: [10.3847/2041-8213/ac2cc1](https://doi.org/10.3847/2041-8213/ac2cc1)

Godfrey, J., Edelman, B., & Farr, B. 2023, *Cosmic Cousins: Identification of a Subpopulation of Binary Black Holes Consistent with Isolated Binary Evolution*, doi: [10.48550/arXiv.2304.01288](https://doi.org/10.48550/arXiv.2304.01288)

Górski, K. M., Hivon, E., Banday, A. J., et al. 2005, *The Astrophysical Journal*, 622, 759, doi: [10.1086/427976](https://doi.org/10.1086/427976)

Graham, M. J., Ford, K. E. S., McKernan, B., et al. 2020, *Physical Review Letters*, 124, 251102, doi: [10.1103/PhysRevLett.124.251102](https://doi.org/10.1103/PhysRevLett.124.251102)

Graham, M. J., McKernan, B., Ford, K. E. S., et al. 2023, *The Astrophysical Journal*, 942, 99, doi: [10.3847/1538-4357/aca480](https://doi.org/10.3847/1538-4357/aca480)

Greene, J. E., & Ho, L. C. 2007, *The Astrophysical Journal*, 667, 131, doi: [10.1086/520497](https://doi.org/10.1086/520497)

—. 2009, *The Astrophysical Journal*, 704, 1743, doi: [10.1088/0004-637X/704/2/1743](https://doi.org/10.1088/0004-637X/704/2/1743)

Greiner, J., Burgess, J. M., Savchenko, V., & Yu, H. F. 2016, *The Astrophysical Journal*, 827, L38, doi: [10.3847/2041-8205/827/2/L38](https://doi.org/10.3847/2041-8205/827/2/L38)

Harris, C. R., Millman, K. J., van der Walt, S. J., et al. 2020, *Nature*, 585, 357, doi: [10.1038/s41586-020-2649-2](https://doi.org/10.1038/s41586-020-2649-2)

Hopkins, P. F., Richards, G. T., & Hernquist, L. 2007, *The Astrophysical Journal*, 654, 731, doi: [10.1086/509629](https://doi.org/10.1086/509629)

Hotokezaka, K., & Piran, T. 2017, *The Astrophysical Journal*, 842, 111, doi: [10.3847/1538-4357/aa6f61](https://doi.org/10.3847/1538-4357/aa6f61)

Hunter, J. D. 2007, *Computing in Science & Engineering*, 9, 90, doi: [10.1109/MCSE.2007.55](https://doi.org/10.1109/MCSE.2007.55)

Ishibashi, W., & Gröbner, M. 2024, *Monthly Notices of the Royal Astronomical Society*, 529, 883, doi: [10.1093/mnras/stae569](https://doi.org/10.1093/mnras/stae569)

Karathanasis, C., Mukherjee, S., & Mastrogianni, S. 2023, *Monthly Notices of the Royal Astronomical Society*, 523, 4539, doi: [10.1093/mnras/stad1373](https://doi.org/10.1093/mnras/stad1373)

Kaspi, S., Smith, P. S., Netzer, H., et al. 2000, *ApJ*, 533, 631, doi: [10.1086/308704](https://doi.org/10.1086/308704)

Klencki, J., Nelemans, G., Istrate, A. G., & Chruslinska, M. 2021, *Astronomy and Astrophysics*, 645, A54, doi: [10.1051/0004-6361/202038707](https://doi.org/10.1051/0004-6361/202038707)

Kunnumkai, K., Palmese, A., Bulla, M., et al. 2024a, arXiv e-prints, arXiv:2409.10651, doi: [10.48550/arXiv.2409.10651](https://doi.org/10.48550/arXiv.2409.10651)

Kunnumkai, K., Palmese, A., Farah, A. M., et al. 2024b, arXiv e-prints, arXiv:2411.13673, doi: [10.48550/arXiv.2411.13673](https://doi.org/10.48550/arXiv.2411.13673)

Li, G.-P. 2022, *Physical Review D*, 105, 063006, doi: [10.1103/PhysRevD.105.063006](https://doi.org/10.1103/PhysRevD.105.063006)

Li, Y.-P., Chen, Y.-X., Lin, D. N. C., & Wang, Z. 2022, *ApJL*, 928, L1, doi: [10.3847/2041-8213/ac5b61](https://doi.org/10.3847/2041-8213/ac5b61)

Ma, Z.-P., Wang, K., Wu, Q., & Wang, J.-M. 2024, Electromagnetic Flares Associated with Gravitational Waves from Binary Black Hole Mergers in AGN Accretion Disks, doi: [10.48550/arXiv.2409.18567](https://doi.org/10.48550/arXiv.2409.18567)

Magaña Hernandez, I., & Palmese, A. 2025a, arXiv e-prints, arXiv:2509.03607, doi: [10.48550/arXiv.2509.03607](https://doi.org/10.48550/arXiv.2509.03607)

—. 2025b, arXiv e-prints, arXiv:2508.19208, doi: [10.48550/arXiv.2508.19208](https://doi.org/10.48550/arXiv.2508.19208)

Magaña Hernandez, I., & Palmese, A. 2025, *Phys. Rev. D*, 111, 083031, doi: [10.1103/PhysRevD.111.083031](https://doi.org/10.1103/PhysRevD.111.083031)

Mandel, I., Farr, W. M., & Gair, J. R. 2019, *Monthly Notices of the Royal Astronomical Society*, 486, 1086, doi: [10.1093/mnras/stz896](https://doi.org/10.1093/mnras/stz896)

Mapelli, M., Bouffanais, Y., Santoliquido, F., Arca Sedda, M., & Artale, M. C. 2022, *Monthly Notices of the Royal Astronomical Society*, 511, 5797, doi: [10.1093/mnras/stac422](https://doi.org/10.1093/mnras/stac422)

Mapelli, M., Santoliquido, F., Bouffanais, Y., et al. 2021, *Symmetry*, 13, 1678, doi: [10.3390/sym13091678](https://doi.org/10.3390/sym13091678)

Marchant, P., Renzo, M., Farmer, R., et al. 2019, *The Astrophysical Journal*, 882, 36, doi: [10.3847/1538-4357/ab3426](https://doi.org/10.3847/1538-4357/ab3426)

McKernan, B., Ford, K. E. S., Callister, T., et al. 2022, *MNRAS*, 514, 3886, doi: [10.1093/mnras/stac1570](https://doi.org/10.1093/mnras/stac1570)

McKernan, B., Ford, K. E. S., Cook, H. E., et al. 2024, McFACTS I: Testing the LVK AGN channel with Monte Carlo For AGN Channel Testing & Simulation (McFACTS), arXiv, doi: [10.48550/arXiv.2410.16515](https://doi.org/10.48550/arXiv.2410.16515)

McKernan, B., Ford, K. E. S., Bartos, I., et al. 2019, *The Astrophysical Journal*, 884, L50, doi: [10.3847/2041-8213/ab4886](https://doi.org/10.3847/2041-8213/ab4886)

McKinney, W. 2010, Proceedings of the 9th Python in Science Conference, 56, doi: [10.25080/Majora-92bf1922-00a](https://doi.org/10.25080/Majora-92bf1922-00a)

Palmese, A., Fishbach, M., Burke, C. J., Annis, J., & Liu, X. 2021, *The Astrophysical Journal*, 914, L34, doi: [10.3847/2041-8213/ac0883](https://doi.org/10.3847/2041-8213/ac0883)

Palmese, A., & Mastrogiovanni, S. 2025, *Encyclopedia of Astrophysics*, Elsevier, arXiv:2502.00239, doi: [10.48550/arXiv.2502.00239](https://doi.org/10.48550/arXiv.2502.00239)

Perna, R., Chruslinska, M., Corsi, A., & Belczynski, K. 2018, *Monthly Notices of the Royal Astronomical Society*, 477, 4228, doi: [10.1093/mnras/sty814](https://doi.org/10.1093/mnras/sty814)

Perna, R., Lazzati, D., & Farr, W. 2019, *The Astrophysical Journal*, 875, 49, doi: [10.3847/1538-4357/ab107b](https://doi.org/10.3847/1538-4357/ab107b)

Raccanelli, A., Kovetz, E. D., Bird, S., Cholis, I., & Muñoz, J. B. 2016, *Physical Review D*, 94, 023516, doi: [10.1103/PhysRevD.94.023516](https://doi.org/10.1103/PhysRevD.94.023516)

Ray, A., Magaña Hernandez, I., Breivik, K., & Creighton, J. 2024, arXiv e-prints, arXiv:2404.03166, doi: [10.48550/arXiv.2404.03166](https://doi.org/10.48550/arXiv.2404.03166)

Rodriguez, C. L., Kremer, K., Chatterjee, S., et al. 2021, *Research Notes of the American Astronomical Society*, 5, 19, doi: [10.3847/2515-5172/abdf54](https://doi.org/10.3847/2515-5172/abdf54)

Rodríguez-Ramírez, J. C., Bom, C. R., Fraga, B., & Nemmen, R. 2024, *Monthly Notices of the Royal Astronomical Society*, 527, 6076, doi: [10.1093/mnras/stad3575](https://doi.org/10.1093/mnras/stad3575)

Rowan, C., Whitehead, H., & Kocsis, B. 2024a, arXiv e-prints, arXiv:2412.12086, doi: [10.48550/arXiv.2412.12086](https://doi.org/10.48550/arXiv.2412.12086)

—. 2024b, arXiv e-prints, arXiv:2412.12086, doi: [10.48550/arXiv.2412.12086](https://doi.org/10.48550/arXiv.2412.12086)

Singer, L. P., Chen, H.-Y., Holz, D. E., et al. 2016, *The Astrophysical Journal*, 829, L15, doi: [10.3847/2041-8205/829/1/L15](https://doi.org/10.3847/2041-8205/829/1/L15)

Spera, M., Mapelli, M., Giacobbo, N., et al. 2019, *Monthly Notices of the Royal Astronomical Society*, 485, 889, doi: [10.1093/mnras/stz359](https://doi.org/10.1093/mnras/stz359)

Stone, N. C., Metzger, B. D., & Haiman, Z. 2017, *Monthly Notices of the Royal Astronomical Society*, 464, 946, doi: [10.1093/mnras/stw2260](https://doi.org/10.1093/mnras/stw2260)

Tagawa, H., Haiman, Z., Bartos, I., & Kocsis, B. 2020a, *The Astrophysical Journal*, 899, 26, doi: [10.3847/1538-4357/aba2cc](https://doi.org/10.3847/1538-4357/aba2cc)

Tagawa, H., Haiman, Z., Bartos, I., Kocsis, B., & Omukai, K. 2021, *Monthly Notices of the Royal Astronomical Society*, 507, 3362, doi: [10.1093/mnras/stab2315](https://doi.org/10.1093/mnras/stab2315)

Tagawa, H., Haiman, Z., & Kocsis, B. 2020b, *The Astrophysical Journal*, 898, 25, doi: [10.3847/1538-4357/ab9b8c](https://doi.org/10.3847/1538-4357/ab9b8c)

Tagawa, H., Kimura, S. S., & Haiman, Z. 2023, *The Astrophysical Journal*, 955, 23, doi: [10.3847/1538-4357/ace71d](https://doi.org/10.3847/1538-4357/ace71d)

Tagawa, H., Kimura, S. S., Haiman, Z., Perna, R., & Bartos, I. 2024, *The Astrophysical Journal*, 966, 21, doi: [10.3847/1538-4357/ad2e0b](https://doi.org/10.3847/1538-4357/ad2e0b)

Tong, H., Fishbach, M., Thrane, E., et al. 2025, arXiv e-prints, arXiv:2509.04151,
doi: [10.48550/arXiv.2509.04151](https://doi.org/10.48550/arXiv.2509.04151)

Vaccaro, M. P., Mapelli, M., Périgois, C., et al. 2024, *Astronomy and Astrophysics*, 685, A51,
doi: [10.1051/0004-6361/202348509](https://doi.org/10.1051/0004-6361/202348509)

Wandel, A., Peterson, B. M., & Malkan, M. A. 1999, *ApJ*, 526, 579, doi: [10.1086/308017](https://doi.org/10.1086/308017)

Wang, J.-M., Liu, J.-R., Ho, L. C., Li, Y.-R., & Du, P. 2021, *The Astrophysical Journal*, 916, L17,
doi: [10.3847/2041-8213/ac0b46](https://doi.org/10.3847/2041-8213/ac0b46)

Wang, M., Ma, Y., Li, H., et al. 2025, *Simulation of Binary-Single Interactions in AGN Disk I: Gas-Enhanced Binary Orbital Hardening*,
doi: [10.48550/arXiv.2501.10703](https://doi.org/10.48550/arXiv.2501.10703)

Whitehead, H., Rowan, C., Boekholt, T., & Kocsis, B. 2024, *Monthly Notices of the Royal Astronomical Society*, 531, 4656, doi: [10.1093/mnras/stae1430](https://doi.org/10.1093/mnras/stae1430)

Zevin, M., Bavera, S. S., Berry, C. P. L., et al. 2021, *ApJ*, 910, 152, doi: [10.3847/1538-4357/abe40e](https://doi.org/10.3847/1538-4357/abe40e)

Zonca, A., Singer, L., Lenz, D., et al. 2019, *The Journal of Open Source Software*, 4, 1298, doi: [10.21105/joss.01298](https://doi.org/10.21105/joss.01298)

7. ACKNOWLEDGEMENTS

We thank Colin Burke, Saavik Ford, Barry McKernan, and Matthew Graham for useful discussion. TC and AP acknowledge that this material is based upon work supported by NSF Grant No. 2308193. This work used resources on the Vera Cluster at the Pittsburgh Supercomputing Center (PSC). We thank the PSC staff for help with setting up our software on the Vera Cluster.

This research has made use of data or software obtained from the Gravitational Wave Open Science Center (gwosc.org), a service of the LIGO Scientific Collaboration, the Virgo Collaboration, and KAGRA. This material is based upon work supported by NSF's LIGO Laboratory which is a major facility fully funded by the National Science Foundation, as well as the Science and Technology Facilities Council (STFC) of the United Kingdom, the Max-Planck-Society (MPS), and the State of Niedersachsen/Germany for support of the construction of Advanced LIGO and construction and operation of the GEO600 detector. Additional support for Advanced LIGO was provided by the Australian Research Council. Virgo is funded, through the European Gravitational Observatory (EGO), by the French Centre National de Recherche Scientifique (CNRS), the Italian Istituto Nazionale di Fisica Nucleare (INFN) and the Dutch Nikhef, with contributions by institutions from Belgium, Germany, Greece, Hungary, Ireland, Japan, Monaco, Poland, Portugal, Spain. KAGRA is supported by Ministry of Education, Culture, Sports, Science and Technology (MEXT), Japan Society for the Promotion of Science (JSPS) in Japan; National Research Foundation (NRF) and Ministry of Science and ICT (MSIT) in Korea; Academia Sinica (AS) and National Science and Technology Council (NSTC) in Taiwan.

Software: astropy ([Astropy Collaboration et al. 2013, 2018, 2022](#)), healpy ([Górski et al. 2005; Zonca et al. 2019](#)), ligo.skymap ([Singer et al. 2016](#)), matplotlib ([Hunter 2007](#)), numpy ([Harris et al. 2020](#)), pandas ([McKinney 2010](#))